20th International Conference on Structural Mechanics in Reactor Technology (SMiRT 20)
Espoo, Finland, August 9-14, 2009
SMiRT 20-Division I, Paper 1917

Two scale damage model for HCF uniaxial and biaxial 304L steel tests

Barbier Gregory[a,b], Desmorat Rodrigue[a], Sermage Jean-Philippe[b] and Courtin Stephan[c]

[a] LMT Cachan, ENS Cachan/CNRS/Université Paris 6/PRES UniverSud Paris, Cachan - France.
barbier@lmt.ens-cachan.fr
[b] EDF R&D / LaMSID, 1 av. Gal de Gaulle, Clamart - France
[c] AREVA NP, Tour AREVA, Paris La Défense - France

Keywords: two scale damage model, biaxial tests, High Cycle Fatigue, 304L steel, cruciform specimen.

1 ABSTRACT

On the idea that fatigue damage is localized at the microscopic scale, a scale smaller than the mesoscopic one of the Representative Volume Element, a three-dimensional two scale damage model has been proposed for High Cycle Fatigue applications and extended to anisothermal cases and to thermo-mechanical fatigue. Mean stress effects are introduced by the consideration of the first stress invariant in the microscale plasticity criterion. The two scale damage model, via the associated fatigue post-processor DAMAGE, was used herein to compare theoretical to experimental number of cycles to rupture on the Electricité de France database made of High Cycle Fatigue uniaxial tests on AISI 304L stainless steel. Then, a thinned Maltese cross specimen was designed and tests were performed to have crack initiation under biaxial loadings. As for 1D tests, calculated and experimental numbers of cycles to crack initiation under biaxial loadings are compared. There is less than a factor 2 between experimental and numerical numbers of cycles to rupture for 1D and biaxial tests.

2 CONTEXT

Some parts of nuclear power plants (mixing tees) are subjected to local thermal-hydraulic phenomena between hot and cold fluids, which could lead to thermo-mechanical fatigue and to crack initiation. Lots of studies have been carried out on this topic. One of the main points is to understand material behaviour under such thermo-mechanical loadings (Pascoe et al. (1967), Samir et al. (2006), Zhang et al. (2007)). Analysis and experimentations have shown that the loading (in mixing tees) is biaxial. In that way, a part of the present work is devoted to a better comprehension of the behaviour of the 304L steel under biaxial loadings thanks to an experimental campaign of High Cycle Fatigue (HCF) biaxial tests performed on a multiaxial device. Another part of the paper is about the application of the two scale damage model (via the post processor DAMAGE) to uniaxial and biaxial tests.

3 TWO SCALE DAMAGE MODEL

On the remark that High Cycle Fatigue, either thermally or mechanically activated, occurs for an elastic regime at the RVE scale, the mesoscale of continuum mechanics, a two scale damage model has been built (Lemaitre et al. (1994)). It accounts for micro-plasticity and micro-damage at the defects scale or microscale. The model is phenomenological, describing micro-plasticity with classical 3D von Mises plasticity equations, describing micro-damage by Lemaitre damage evolution law $\dot{D} = \left(\frac{Y}{S}\right)^{s} \dot{p}$ of damage governed by the accumulated plastic strain rate $\dot{p}$, with Y the elastic energy density and S and s as damage parameters. A scale transition law makes the link between both mesoscopic and microscopic scales (Fig.1).
The general principles for building a two scale damage model for thermal and/or thermo-mechanical fatigue are as follows,

- at the mesoscale, the scale of the RVE of continuum mechanics, the behaviour is considered as thermo-elastic, the material engineering yield stress $_y$ being usually not reached in High Cycle Fatigue (accordingly called elastic fatigue),
- the microscale is the defects scale, defects conceptually gathered as a weak inclusion imbedded in previous RVE. The behaviour at microscale is thermo-elasto-plasticity coupled with damage, the weakness of the inclusion being represented by a yield stress at microscale $_y$ taken equal to the asymptotic fatigue limit of the material $_f^\infty$.

At the mesoscale, the stresses are denoted , the total, elastic and plastic strains are , ^{e}, ^{p}. They are known from a thermo-elastic Finite Element (FE) computation as for High Cycle Fatigue one has most often $^p \approx 0$. An initial hardening can be handled by the two scale damage model by considering constant non zero mesoscopic plastic strains ^{p} -- for instance gained from the nonlinear FE analysis of the initial yielding.
The values at the microscale have an upper-script . For High Cycle Fatigue, with plasticity and damage assumed to occur at the microscale only, one has $^p \neq 0$, $0 < D < 1$, where for simplicity the damage variable at the microscale has no upper-script (D=D).

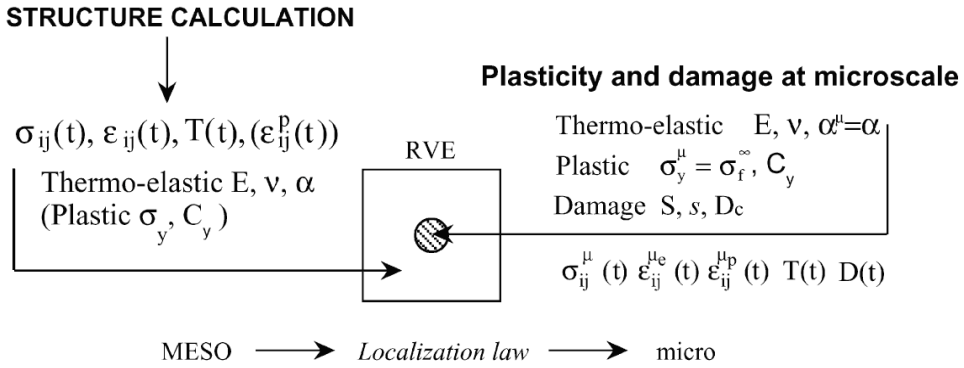

Figure 1. Micro element imbedded in a thermo-elastic Representative Volume Element.

3.1 Thermo-elastic behaviour at mesoscale

The thermoelastic law for the RVE reads

$$\boldsymbol{\epsilon}^e = \frac{1+\nu}{E}\boldsymbol{\sigma} - \frac{\nu}{E}\mathrm{tr}\,\boldsymbol{\sigma}\,\mathbf{1} + \alpha(T - T_{\mathrm{ref}})\mathbf{1}$$

with E the Young modulus, the Poisson ratio, the thermal expansion coefficient and T_{ref} the reference temperature. The non homogeneous temperature and eventually time dependent field in a structure T(x,t) is usually determined from an initial heat transfer computation. The mechanical properties E, , may depend on the temperature. The shear and bulk modulus of the material will respectively be G=E/2(1+) and K=E/3(1-2).

3.2 Plasticity and damage at microscale

A law of thermo-elasto-plasticity coupled with damage is considered at microscale. No viscosity is considered as for the applications in mind the temperature will remain much lower than one third of the melting temperature. The elasticity law reads then (recall that -upper-script stands for "variable at microscale"):

$$\boldsymbol{\epsilon}^{\mu e} = \frac{1+\nu}{E}\frac{\boldsymbol{\sigma}^\mu}{1-D} - \frac{\nu}{E}\frac{\mathrm{tr}\,\sigma^\mu}{1-D}\mathbf{1} + \alpha^\mu(T - T_{\mathrm{ref}})\mathbf{1}$$

where the thermal expansion coefficient is taken next equal to the meso coefficient . In the yield criterion, the hardening **X** is kinematic, linear, and the yield stress is the asymptotic fatigue limit of the material, denoted $_f^\infty$,

$$f^\mu = (\tilde{\boldsymbol{\sigma}}^\mu - \boldsymbol{X}^\mu)_{eq} + kTr\tilde{\boldsymbol{\sigma}}^\mu - \sigma_f^\infty$$

with *Tr(.)* the first stress invariant of the stress at micro scale, and *k* a Drucker-Prager parameter (Drucker et al. (1952)) to identify (Barbier et al. (2008)), $(.)_{eq}$ von Mises norm and where the elasticity domain is defined by f <0.
The set of constitutive equations at microscale is then:

$$
\begin{cases}
\boldsymbol{\epsilon}^{\mu} = \boldsymbol{\epsilon}^{\mu e} + \boldsymbol{\epsilon}^{\mu p}, \\
\boldsymbol{\epsilon}^{\mu e} = \dfrac{1+\nu}{E}\tilde{\boldsymbol{\sigma}}^{\mu} - \dfrac{\nu}{E}\operatorname{tr}\tilde{\boldsymbol{\sigma}}^{\mu}\mathbf{1} + \alpha(T - T_{\text{ref}})\mathbf{1}, \\
\dot{\boldsymbol{\epsilon}}^{\mu p} = \dfrac{3}{2}\dfrac{\tilde{\boldsymbol{\sigma}}^{\mu D} - \boldsymbol{X}^{\mu}}{(\tilde{\boldsymbol{\sigma}}^{\mu} - \boldsymbol{X}^{\mu})_{\text{eq}}}\dot{p}^{\mu}, \\
\dfrac{\mathrm{d}}{\mathrm{d}t}\left(\dfrac{\boldsymbol{X}^{\mu}}{C_y}\right) = \dfrac{2}{3}\dot{\boldsymbol{\epsilon}}^{\mu p}(1-D), \\
\dot{D} = \left(\dfrac{Y^{\mu}}{S}\right)^{s}\dot{p}^{\mu} \quad \text{if} p^{\mu} > p_D^{\mu} \text{ or if } w_s^{\mu} > w_D, \\
D = D_c \rightarrow \text{crack initiation}
\end{cases}
$$

with the plastic modulus C_y, the damage strength S, the damage exponent s as temperature dependent material parameters.
In previous laws, p is the accumulated plastic strain at microscale, w_s is the stored energy density and p_D and w_D are the corresponding damage thresholds. A damage threshold in terms of accumulated plastic strain is loading dependent so that a threshold in terms of stored energy can advantageously be considered. A crack is initiated when D reaches the critical damage D_c.

3.3 Localization law coupled with damage and temperature

The scale transition meso → micro is governed by modified Eshelby-Kröner localization law (Eshelby (1957), Kröner (1962), Seyedi et al. (2004)):

$$\boldsymbol{\epsilon}^{\mu D} = \frac{1}{1-bD}\left[\boldsymbol{\epsilon}^{D} + b\left((1-D)\boldsymbol{\epsilon}^{\mu p} - \boldsymbol{\epsilon}^{p}\right)\right],$$

$$\epsilon_H^{\mu} = \frac{1}{1-aD}\left[\epsilon_H + a\left((1-D)\alpha^{\mu} - \alpha\right)(T - T_{\text{ref}})\right]$$

Where $(.)^D=(.)-(1/3)\text{tr}(.)\mathbf{1}$ stands for the deviatoric part of a tensor, $(.)_H=(1/3)\text{tr}(.)$ for the hydrostatic part. By considering $= {}^{D} + {}_{H}\mathbf{1}$, ${}^{D} + {}_{H}\mathbf{1}$ the localization law reads:

$$\boldsymbol{\epsilon}^{\mu} = \frac{1}{1-bD}\left[\boldsymbol{\epsilon} + \frac{(a-b)D}{3(1-aD)}\operatorname{tr}\boldsymbol{\epsilon}\mathbf{1} + b\left((1-D)\boldsymbol{\epsilon}^{\mu p} - \boldsymbol{\epsilon}^{p}\right)\right] + \frac{a((1-D)\alpha^{\mu} - \alpha)}{1-aD}(T - T_{\text{ref}})\mathbf{1}$$

with *a* and *b* the Eshelby parameters for a spherical inclusion,

$$a = \frac{1+\nu}{3(1-\nu)}, \qquad b = \frac{2}{15}\frac{4-5\nu}{1-\nu}$$

3.4 Fatigue post-processor

The equations of the two scale damage model are implemented in a fatigue post-processor DAMAGE_2005 (Desmorat et al. (2007)). The current release of the post-processor is called DAMAGE.
This post-processor is a Fortran program which solves explicitly the two scale damage model constitutive equations with an Euler backward scheme. A graphical interface makes the software use quite easy. For a given material parameters file and for a given loading sequence, the program calculates the time to crack initiation, i.e. the time to reach the critical damage D_c. The inputs are either 1D or come from any 3D Finite Element computations.

4 BULK INITIATION OF CRACK IN BIAXIAL FATIGUE TESTS

4.1 Uniaxial tests for parameters identification

Uniaxial tests were performed by EDF R&D on classical 1D specimen. These tests were strain controlled, performed at room temperature. The strain ratio was equal to -1 (tension-compression tests) and the strain rate was fixed to $4.10^3 s^{-1}$ (Le Roux 2004). They have been used to identify the model material parameters.

4.2 Biaxial tests on thinned Maltese cross shaped specimen

4.2.1 Experimental set up

A thinned Maltese cross specimen has been designed (Fig. 2) thanks to Finite Element Cast3m code and DAMAGE post-processor. This specimen is made to initiate HCF crack on its central area under various (proportional, non proportional) biaxial loadings. The tests are carried out on a multiaxial testing machine (ASTREE) at LMT Cachan. This testing machine has six servohydraulic actuators. The four horizontal actuators used herein have a 100 kN load capacity and a 250 mm stroke range.

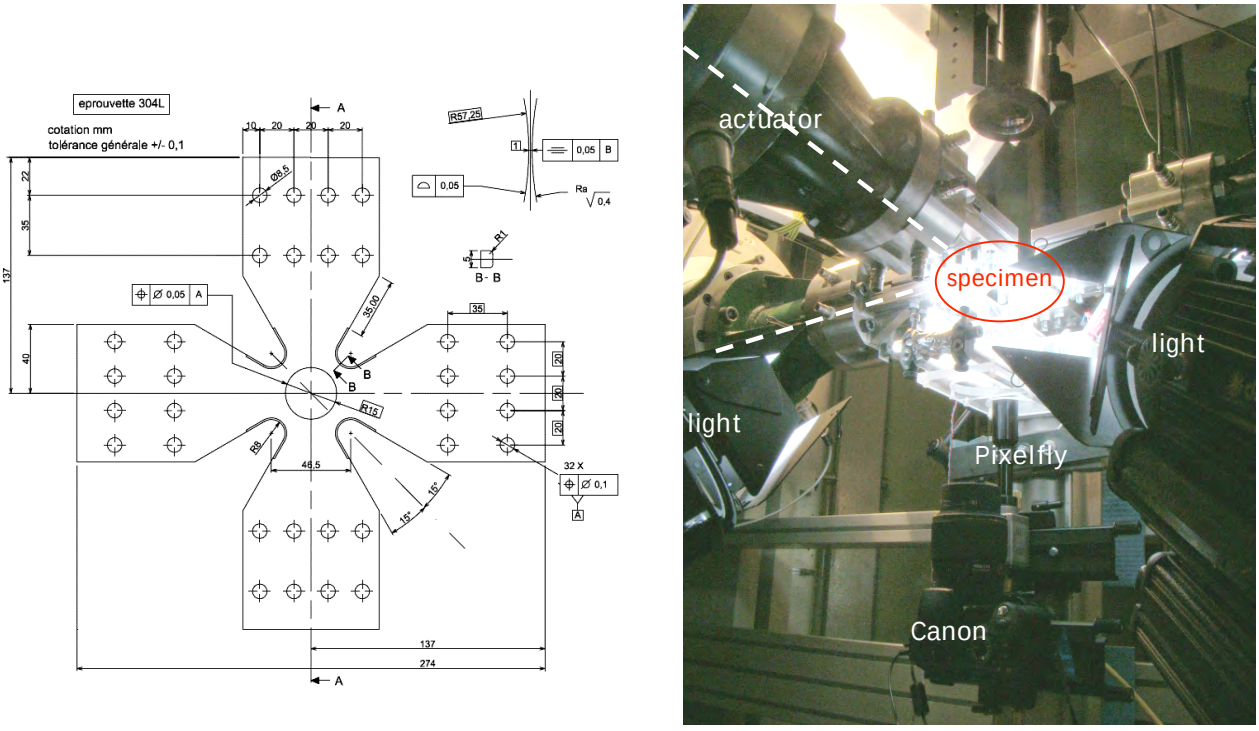

Figure 2. Geometry of the specimen. General view of a biaxial test.

Biaxial tests are load controlled and are performed at room temperature at a frequency of 10Hz. Most of the tests are made with a 0.1 load ratio: due to the behaviour of the material, permanent strains in central area could reach about 10%. In those conditions it's impossible to use classical stain gauges and that is why image correlation (Correli^{LMT} (Besnard et al. 2006)), is used to follow crack initiation and history of strain fields.

Strain fields are monitored using different cameras. About fifteen biaxial tests were performed, various kinds of experimental set up were tested but the general idea is as follow:

- determination of the localisation and the evolution of the crack as well as the evolution of plastic strains in the entire specimen: a numerical camera (Canon EOS 350D, 3456 x 2304 pixels) is used to acquire all the geometry of the specimen. Images corresponding to F=0 and F=Fmax loads at typically all the 10^4 cycles are taken.
- determination of the stress amplitude of the central area submitted to biaxial loading during experiment conditions: a CCD camera (PCO Pixelfly, 1360 x 1024 pixels, 12 bits) with telecentric objective x1 (Edmunds Optic) is used for stroboscopic acquisition.

4.2.2 Results and discussions

Performed tests could be divided into three kinds of various loadings:

- Tests A, B, C, D and H correspond to equibiaxial loadings ($F_1 = F_2$) at a load ratio $R_F=F_{min}/F_{max}=0.1$.
- Test I is equibiaxial with a load ratio $R_F=-1$.

- Tests E, F and G correspond to F_1 cyclic (load ratio R_F=0.1) and F_2 constant. For the three tests, F_1=38kN, whereas F_2 respectively equals 38kN, 19kN and 0kN for E, F and G tests.

To have a scalar used to compare uniaxial and biaxial tests, the maximum of stain amplitude loading is chosen. For equibiaxial tests, we have (direction 33 is the out of plane direction):

$$\Delta\varepsilon_{33}=-\frac{2\nu}{E}\Delta\sigma_{11} \text{ et } \Delta\varepsilon_{11}=\Delta\varepsilon_{22}=\frac{1-\nu}{E}\Delta\sigma_{11}$$

$$\Delta\varepsilon_{33}=2\frac{\nu}{\nu-1}\Delta\varepsilon_{11}\ .$$

As the real material behaviour is between a pure elastic (i.e. =0.3) and a plastic one (i.e. =0.5), we finally have:

$$0,85\times\Delta\varepsilon_{11}\leq\Delta\varepsilon_{33}\leq 2\times\Delta\varepsilon_{11}$$

Consequently, the maximum strain amplitude loading is between $_{11}$ and 2 $_{11}$. This is why errors bars are plotted in Fig.4 which summarizes results of stress and strain controlled uniaxial tests (stress controlled tests were performed on a 304L Thyssen steel, different from the 304L CLI steel used for the other tests) and the biaxial tests performed for this study. For biaxial tests, number of cycles to rupture is said to be the moment when we have crack initiation observed thanks to image correlation (Fig.3).

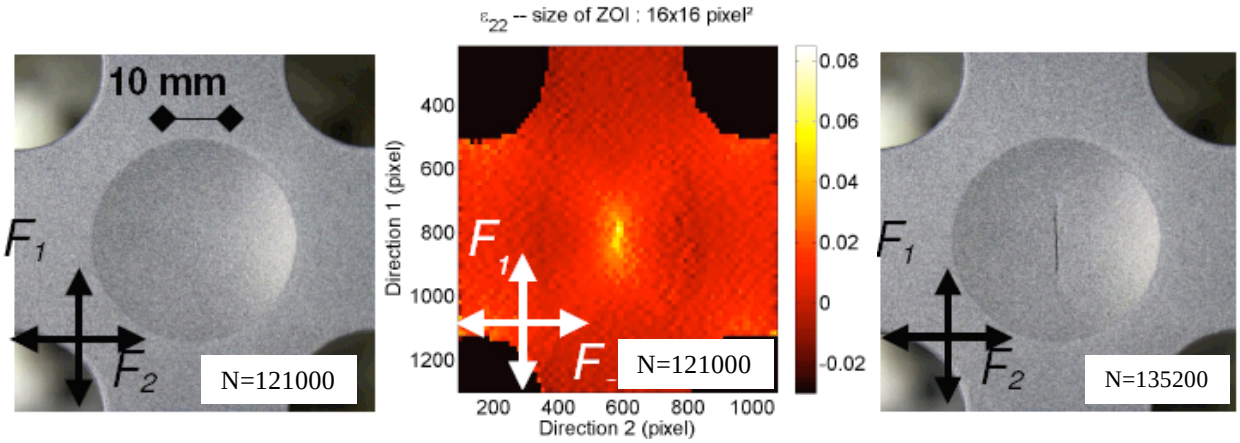

Figure 3. View of the specimen at 121000 cycles (image correlation indicates a high strain loaded area) and view at 135200 cycles when the crack is open.

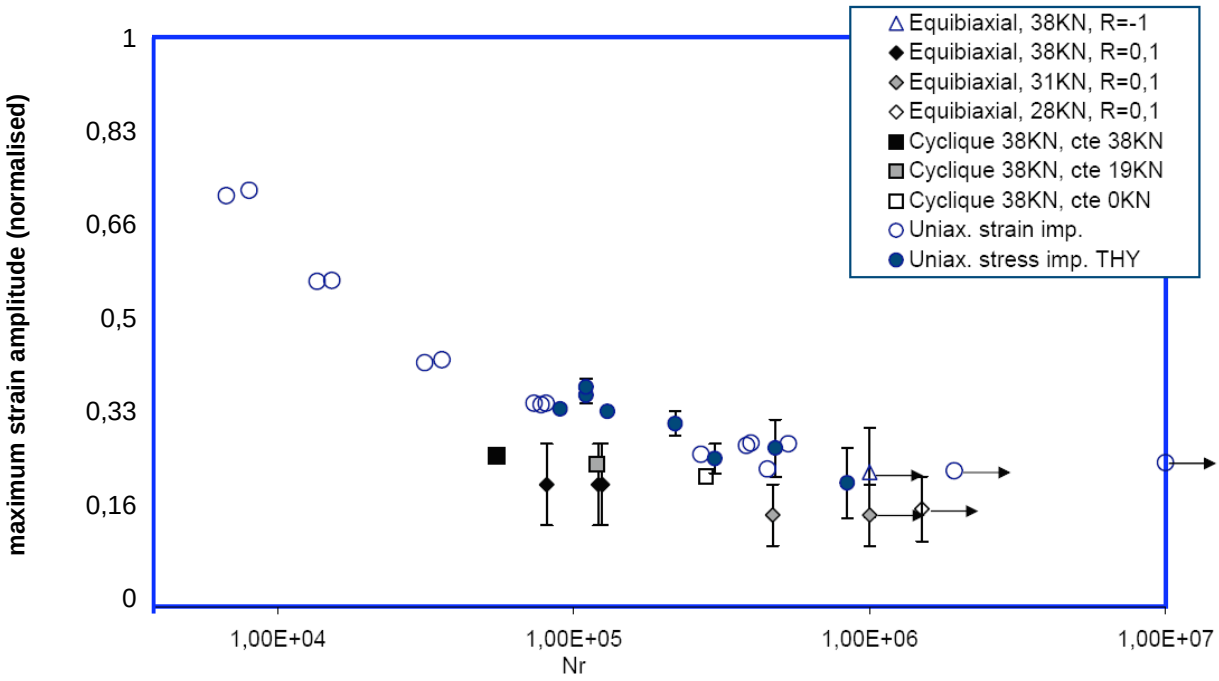

Figure 4. Summary of biaxial fatigue results.

We can observe that :

- Multiaxial loading does not seem to be more damageable than uniaxial loadings (the R=-1 loading is very close to uniaxial points). But as there is just one point for multiaxial R=-1 configuration, we cannot conclude positively now.
- Mean stress effect on life is clearly visible. Life of tests submitted to a loading with high mean stress (tests A,B,C,D,E,F,G and H) have a shorter life than uniaxial points (performed at R=-1)

5 DAMAGE FATIGUE POST-PROCESSOR

5.1 Material parameters identification

The material parameters to identify are: the Young modulus E, the Poisson coefficient , the thermal expansion coefficient , the yield stress $_y$, the plastic modulus C_y, the ultimate stress $_u$, the asymptotic fatigue limit $^{\infty}_f$, and the damage parameters S, s, Dc, h (for metals, h=0.2).
Uniaxial strain controlled tests are used for the identification of the damage parameters. Values of imposed strains are multiplied by Young modulus of the material for the identification in the post processor (pure elastic behaviour assumption). Obtained curves are then divided by the Young modulus so as to have original values. The identifications for three temperatures (room temperature, 150°C and 300°C) are presented in Fig. 5 and parameters are summarized in Table 1.

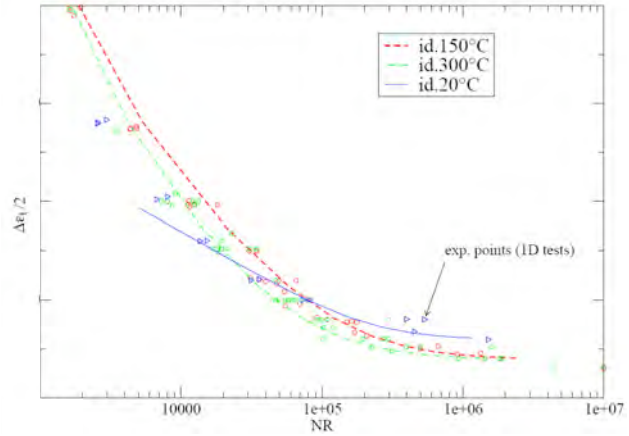

Figure 5. Identifications for 3 temperatures.

Table 1. Parameters used for DAMAGE post-processor

T (°C)	E (GPa)	Cy (MPa)	(l/°C)	S (MPa)	s	f^{∞} (MPa)
20	197	1740	$1.652\ 10^{-5}$	1.7	3.5	295
150	188	1824	$1.762\ 10^{-5}$	50	1.2	187
300	176	1910	$1.884\ 10^{-5}$	100	1.0	175

5.2 Results and discussions

DAMAGE post processor is used to calculate the number of cycles to rupture (NR) for various loadings.
First of all, the uniaxial strain controlled tests of the EDF database are studied. Applied strains are directly the inputs for the post processor. The following figure (Fig.6) shows comparisons between experimental NR and numerical NR obtained by DAMAGE post-processor. Not all the experimental results are computed, but just a few in the HCF zone (i.e. NR>10^5 cycles).
Then, biaxial tests performed at LMT Cachan are studied. As said previously, those tests were load controlled but the strain amplitudes in the centre of the specimen were constant for the main part of the tests. So it seems correct to say that the area submitted to biaxial loading is quasi strain controlled. Those strain amplitudes (measured thanks to image correlation) are the inputs for DAMAGE post-processor. Different biaxial tests are compared: tests E, F and G (corresponding to F_1 cyclic (load ratio R_F=0.1) and F_2 constant), tests I and H (where a first equibiaxial loading at 31kN leaded to non failure of the specimen, then a second loading at 38kN was applied during about 10^5 cycles (rupture)).
It can be seen that all the numerical calculated NR are in a scatter of 2 compared with experimental points. Except for points corresponding to NR<10^5 cycles, the two scale damage model is conservative.

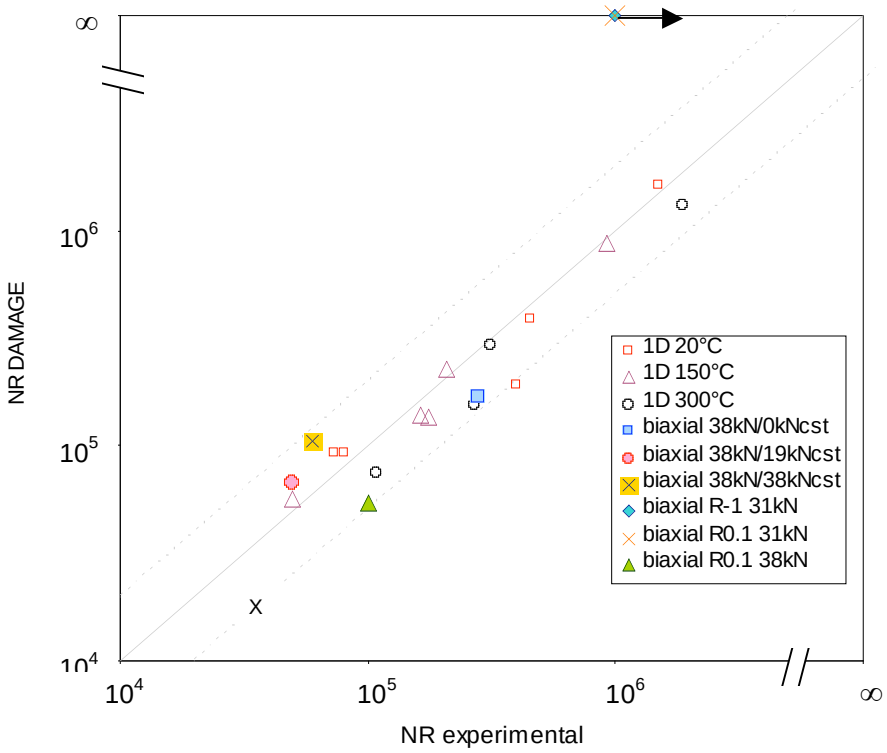

Figure 6. Comparison between experimental and numerical numbers of cycles to rupture.

6 CONCLUSION

The two scale damage model developed in LMT-Cachan and implemented in a fatigue post-processor (DAMAGE) is used herein to calculate the number of cycles to rupture of uniaxial fatigue tests performed by EDF R&D and biaxial tests performed at LMT-Cachan on a 304L AISI steel. A cross specimen has been designed for this study and various biaxial fatigue loadings were applied, cracks having well initiated in the specimen centre (bulk initiation). Image correlation was used to measure characteristics of the biaxial tests (i.e. strain amplitudes, history of plastic strains, initiation). There is less than a factor 2 between experimental and numerical numbers of cycles to rupture.

Acknowledgements. *Authors would like to acknowledge EDF, CEA, AREVA NP, SNECMA Space Engine Division SAFRAN Group and CNES for their financial and scientific supports.*

REFERENCES

Barbier G., Desmorat R., Sermage J.P., du Tertre A. and Courtin S. 2008. Mean stress effect by incremental two scale damage model. In Proc. LCF6 Berlin.

Besnard G., Hild F., and Roux S. 2006. *Exp. Mech.*, 46(6), 2006, 789–804.

Desmorat R. et al. 2007. Two scale damage model and related numerical issues for thermo-mechanical High Cycle Fatigue, Eur. Jour. of Mech. A/Solids, Vol. 26, pp. 909-935.

Drucker D. C. and Prager W. 1952. Soil Mechanics and Plastic Analysis of Limit Design, Quart. Applied Mathematics, Vol.10, No.2.

Eshelby, J.D. 1957. The determination of the elastic field of an ellipsoidal inclusion, related problems. Proc. Roy. Soc. London Ser. A 241, 376.

Kröner, E. 1961. On the plastic deformation of polycrystals. Acta Metall. 9, pp.155–161.

Lemaitre J., Doghri I. 1994. Damage 90: a post-processor for crack initiation. Comp. Methods Appl. Mech. Engrg. 115: 197-232..

Le Roux J-.C. 2004. Influence de paramètres métallurgiques et d'essai sur l'amorçage des fissures de fatigue en déformation imposée des aciers inoxydables austénitiques. EDF R&D HT-26/03/056/B report.

Pascoe K. J. de Villiers J. W. R. 1967. Low cycle fatigue of steels under biaxial straining, Jour. of Strains Analysis vol. 2 no 2.

Samir A.,Simon A.,Scholz A.,Berger C., 2006, Service-type creep-fatigue experiments with cruciform specimens and modelling of deformation. Int. Jour. of Fatigue 28 643–651.

Seyedi, M., Desmorat, R., Sermage, J.-P. 2004. A two scale model for thermo-mechanical high cycle fatigue failure. In: European Conference on Fracture ECF 15, Advanced Fracture Mechanics for Life and Safety, Stockholm, Sweden.

Zhang S., Sakane M. 2007, 2199 Multiaxial creep–fatigue life prediction for cruciform specimen. Int. Jour. of Fatigue 29 2191.